

Noise and Fluctuations in Nanowire Biosensors

Gerhard Tulzer* Clemens Heitzinger*,**

* Vienna University of Technology, Wiedner Hauptstrasse 8-10, A-1040 Vienna, Austria. (e-mail: gerhard.tulzer@tuwien.ac.at).

** School of Mathematical and Statistical Sciences, Arizona State University, Tempe, AZ 85287, USA

Abstract: This work deals with the stochastic simulation of a nanowire biosensor surface and the surrounding liquid domain for DNA detection. The objective is an analysis of the fluctuations and of the biological noise induced by the inherent randomness of the hybridization process at the surface. We consider a coupled system of diffusion-reaction equations to model the movement of DNA oligomers as well as the hybridization processes at the functionalized surface of the sensor. Since analytical solutions cannot be derived, numerical investigation is necessary. Here, we present an algorithm different from the already published one in Tulzer and Heitzinger (2014) and show the non-monotonic behaviour of the variance in certain regimes. The variance determines the detection limit, which is an important quantity for optimal sensor design.

Keywords: DNA hybridization, nanowire biosensor, stochastic processes.

1. INTRODUCTION

The applicability of nanowire field-effect sensors for the detection of several types of biomolecules in liquids has been shown experimentally, assuring fast, efficient and label-free detection (Zheng et al., 2005; Patolsky et al., 2006; Stern et al., 2007, 2010; Hunt and Armani, 2010; Duan et al., 2012). However, the optimal design of the sensor is still a main topic of research. We have developed mathematical models for the average sensor response (Baumgartner et al., 2011b,a; Baumgartner and Heitzinger, 2012; Baumgartner et al., 2012, 2013) and for the surface processes at biosensors (Bulyha and Heitzinger, 2011) as well as for gassensors (Tulzer et al., 2013), which provided insights into the rational design of the sensors.

The hybridization and dissociation processes taking place at a nanowire biosensor surface give rise to *biological noise* (Hassibi et al., 2004, 2005, 2007; Das et al., 2009; Deen et al., 2006) and should therefore be considered as stochastic processes to take into account their random nature. These equations are coupled to a diffusion equation in the liquid phase surrounding the surface to model the limited transport of DNA oligomers in the liquid phase. This coupled model also reflects the small amount of target molecules present in the simulation domain. Since hybridization and diffusion occur at the same timescale, the whole system is considered in a stochastic formulation.

Recently, we followed a box approach to realize the coupled system of equations, which allowed the prediction of several important quantities like signal-to-noise ratio and response time (Tulzer and Heitzinger, 2014). Here, we

employ a random walk approach to simulate the system, which turns out to be computationally more efficient.

The paper is organized as follows: In Section 2, the hybridization model is described, and some analytical results for simplified cases are given. In Section 3, the coupling of the diffusion equation to the hybridization is explained. The algorithm implemented for the simulations is considered in Section 4, and numerical results are presented in Section 5.

2. THE HYBRIDIZATION MODEL

We consider the hybridization of DNA on a nanowire sensor surface. The latter has been functionalized with probe molecules. The hybridization and dissociation processes at the surface considered in this study are



where \mathbf{T} denotes a target molecule, \mathbf{P} denotes a probe molecule and \mathbf{PT} denotes a probe-target complex at the sensor surface and r_a and r_d are the hybridization and the dissociation rate, respectively. Numerical values for these quantities have been estimated in (Tulzer and Heitzinger, 2014) for different probe densities, which will be used for simulations in this work.

Assuming large but constant amounts of target as well as probe molecules and also considering a reservoir of target molecules, the processes stated above are described by an ordinary differential equation,

* The authors acknowledge support by the FWF (Austrian Science Fund) START project no. Y660 *PDE Models for Nanotechnology*.

$$\frac{d\mathbf{PT}}{dt}(t) = r_a C_T (C_P - \mathbf{PT}(t)) - r_d \mathbf{PT}(t) \quad (3)$$

$$\mathbf{PT}(0) = 0, \quad (4)$$

where C_T and C_P are the concentrations of the target and probe molecules, respectively. This differential equation can easily be solved analytically assuming that C_T is constant.

However, when dealing with nanostructures, one is interested in small amounts of particles, in which case it is inappropriate to neglect the random character of the investigated processes. We model both surface reactions as stochastic processes, which is an approach yielding a chemical Langevin equation for the system (Gillespie, 2008). The number \mathbf{PT} of probe-target complexes then becomes a random variable. The number of reactions taking place in a time interval τ is a counting process and therefore obeys Poisson distributions with the parameters

$$a(\mathbf{PT}_t, \tau) = \tau r_a C_T (C_P - \mathbf{PT}_t) \quad (5)$$

$$d(\mathbf{PT}_t, \tau) = \tau r_d \mathbf{PT}_t \quad (6)$$

for the association and the dissociation process, respectively. However, when considering large enough time intervals τ , the Poisson distribution can be approximated by a normal distribution with the same mean and variance (Higham, 2008).

With this, the chemical Langevin equation in white-noise form becomes

$$d\mathbf{PT}_t = (r_a C_T (C_P - \mathbf{PT}_t) - r_d \mathbf{PT}_t) dt + \sqrt{r_a C_T (C_P - \mathbf{PT}_t)} dB_1 - \sqrt{r_d \mathbf{PT}_t} dB_2, \quad (7)$$

$$\mathbf{PT}_0 = 0,$$

where dB_1 and dB_2 are two independent Wiener processes.

Under the simplifying assumption of constant amounts of target molecules throughout the liquid, the expected value and the variance are calculated from the Langevin equation as

$$\mathbb{E}(\mathbf{PT}_t) = \frac{\alpha}{\beta} (1 - e^{-\beta t}), \quad (8)$$

$$\mathbb{V}(\mathbf{PT}_t) = \frac{\alpha}{\beta^2} (1 - e^{-\beta t}) (r_d + r_a C_T e^{-\beta t}), \quad (9)$$

where $\alpha := r_a C_P C_T$ and $\beta := r_a C_T + r_d$ (Tulzer and Heitzinger, 2014).

3. THE COUPLED MODEL

When considering nanostructures, the modeling of the target molecule density to be constant is not very accurate. In fact, it is more reasonable to consider the number of target molecules to be limited and to consider them as particles diffusing through the liquid domain. The concentration of target molecules $u(x, t)$ throughout the liquid is governed by the diffusion equation

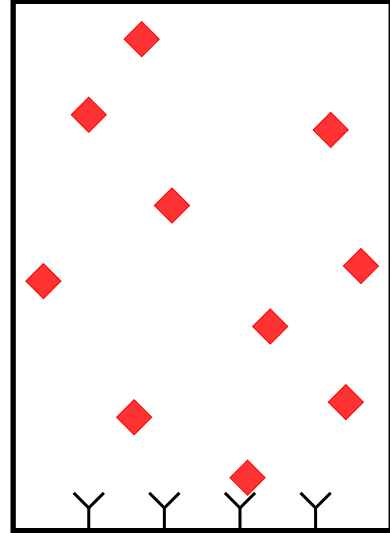


Fig. 1. Sketch of the domain. The Y-shaped objects are the probe molecules and the red diamonds represent the target molecules. The whole domain is partitioned in several boxes according to the simulation algorithm described in the text.

$$\frac{\partial u}{\partial t} = D \Delta u \quad \text{in } \Omega \times (0, T], \quad (10)$$

$$\nu \cdot \nabla u = g \quad \text{on } \partial\Omega \times (0, T], \quad (11)$$

$$u(x, 0) = u_0 \quad \text{in } \Omega. \quad (12)$$

The function g models the hybridization at the sensor surface as well as homogeneous Neumann conditions at all the other boundaries. Now, $C_T(t) := u(\partial\Omega_s, t)$ is the mean concentration at the surface. Here, we are only considering a 1D domain, because diffusion in all directions parallel to the surface has no influence on the outcome of the simulation. This is due to the fact that we are considering a uniform surface, so that adsorption is equally likely everywhere. As in Tulzer and Heitzinger (2014), the diffusion constant is chosen to be $D = 8.8775 \cdot 10^{-11} \text{ m}^2/\text{s}$.

The coupling with the hybridization-diffusion process is achieved via the boundary condition at the sensor surface.

3.1 Signal-to-Noise ratio

The signal-to-noise ratio is an important quantity in sensor design, since it is a measure for the quality of a signal and determines the threshold for distinguishing it from noise. Its value is given by

$$\text{SNR}(t) := \frac{\mathbb{E}(X_t)}{\sqrt{\mathbb{V}(X_t)}}. \quad (13)$$

This ratio is a dimensionless value.

Of course, a high signal-to-noise ratio is always desired.

4. ALGORITHM

In Tulzer and Heitzinger (2014), we employed a box transition algorithm for the diffusion to simulate the coupled system of equations. Here, we present an algorithm based on random walks, which was proposed in Erban et al. (2007). In every step, the particles are moved randomly

according to their diffusion constant. Moreover, for every particle near the surface a random number decides whether the target molecule binds to the surface. Also, for every probe-target complex, a random number decides whether the hybridized complex dissociates. Summarizing, the algorithm is the following:

- (1) Place target molecules in the box according to the desired initial condition.
- (2) Move every particle in the domain according to

$$X_i(t + \Delta t) = X_i(t) + \sqrt{2D\Delta t}\xi, \quad (14)$$

where ξ is a random number drawn from a Gaussian distribution. Use reflective boundary conditions for the molecules that would otherwise move outside the box.

- (3) For every target molecule near the surface, draw a random number η from a uniform distribution and consider the respective particle hybridized if

$$\eta \leq r_a C_T(t) (C_P - \mathbf{PT}(t)) \Delta t, \quad (15)$$

where C_T here denotes the concentration of target molecules near the surface.

- (4) For every hybridized complex, draw a random number ζ from a uniform distribution. If

$$\zeta \leq r_d \mathbf{PT}(t) \Delta t, \quad (16)$$

consider the complex dissociated and insert a particle in the liquid near the surface.

- (5) Unless final time t_{end} is reached, go to step (2).

To obtain the statistics for surface hybridization, the algorithm needs to be repeated many times in order to calculate the necessary moments. Parallelization is straightforward, since every run is independent of all the others. Therefore, one can distribute the total amount of evaluations onto several cores, which can be easily implemented in MATLAB by using the *parfor* command instead of the usual *for* command.

One important reason to employ the random walk approach is the savings in computational effort. Moreover, another favorable aspect for the random-walk algorithm is its simple extendability to higher dimensions, which would have been quite awkward in the box-based approach.

5. NUMERICAL RESULTS

The simulations were performed for 2×10^{12} probe molecules per cm^2 , for which the surface reaction rates have been determined in Tulzer and Heitzinger (2014).

5.1 Comparison to the Box-Based Algorithm

First, we show the equivalency to the box-based algorithm. We performed a simulations with a $1 \mu\text{M}$ solution of target molecules in the liquid. The comparison of the mean value and the variance is shown in Figure 2. The agreement of both simulations validates the random-walk approach.

As mentioned, this algorithm is favorable due to the savings in computation time. In our experiments, the random-walk based algorithm was approximately five times faster than the box-based algorithm. Since parallelization only means that we distribute the single evaluations on several cores, this result is independent of the number of cores we

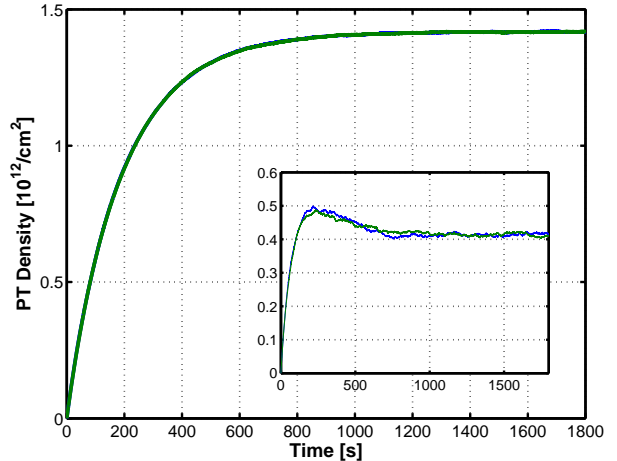


Fig. 2. Comparison of the results of the two different algorithms. The green line represents the random-walk-based algorithm, while the blue line represents the box-based algorithm. The main frame shows the mean value, while the inset shows the variance.

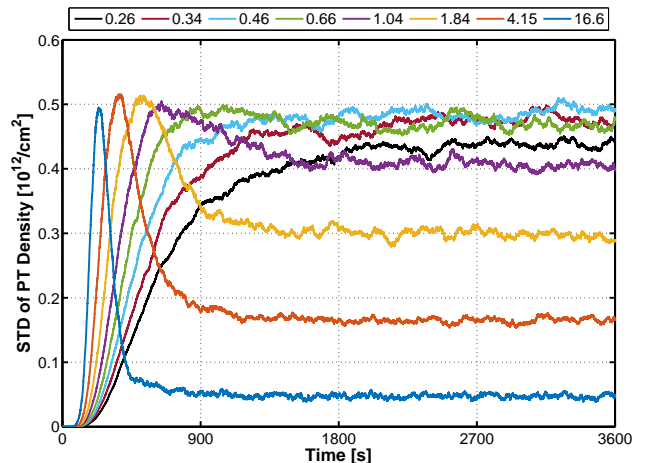


Fig. 3. Evolution of the variance for different target molecule densities, given in μM . At higher target molecule densities, the variance is not monotone and shows a maximum after a certain period of time depending on the concentration.

are using, as long as we use the same number for both algorithms.

5.2 Behaviour of the Variance

The variance of the PT-density is zero at $t = 0$ by definition of the initial conditions of the system. Its evolution over time shows some very interesting properties in certain regimes, where one encounters a significant maximum after a certain period of time and the final equilibrium is reached at a lower value. The exact shape for different target molecule densities can be seen in Figure 3. This phenomenon arises at higher target molecule concentrations and breaks down at approximately $0.5 \mu\text{M}$. To the best of our knowledge, this effect has not been reported in the literature so far.

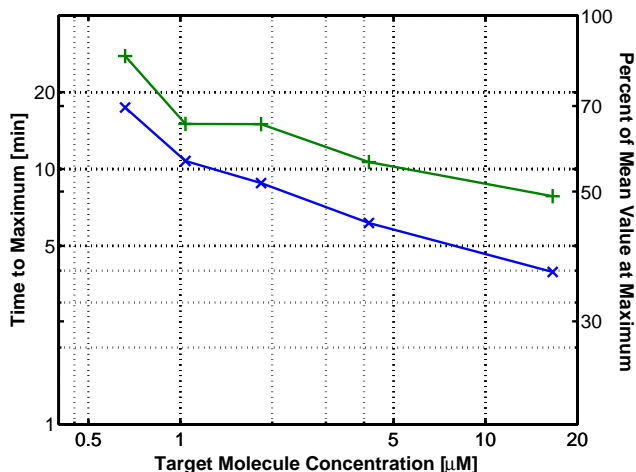


Fig. 4. Blue curve: Time until maximum in Variance is reached (left y -axis). Green curve: Percent of maximum mean value when the maximum in variance is reached (right y -axis).

In the non-monotonic cases the period of time until the maximum is reached varies with target molecule density. Also, the mean value percentage at the variance maximum (with respect to the final value) decreases with target molecule concentration. This means that the waiting time for the best signal-to-noise ratio increases with increasing target molecule density, since after the variance maximum is reached, the signal still increases and the variance will decrease. Both values are shown in Figure 4.

6. CONCLUSIONS

We presented a random-walk based algorithm for the simulation of coupled system of diffusion reaction equations to model the hybridization kinetics at nanowire biosensor surfaces. Its favorable features are speed and easy extendability to higher dimensions. For example, more realistic geometries as well as more complicated initial conditions could be implemented to further increase the applicability of the simulations.

We also showed that the biological noise evolution is not monotone in certain regimes, which is an important fact regarding the optimal sensor design, since the signal-to-noise ratio depends heavily on the noise. Therefore, this kind of simulations makes it possible to determine the optimal device parameters, including the probe density, for each use case. This enables rational design of this type of biosensors.

REFERENCES

Baumgartner, S. and Heitzinger, C. (2012). Existence and local uniqueness for 3d self-consistent multiscale models for field-effect sensors. *Commun. Math. Sci.*, 10(2), 693–716.

Baumgartner, S., Heitzinger, C., Vacic, A., and Reed, M.A. (2013). Predictive simulations and optimization of nanowire field-effect PSA sensors including screening. *Nanotechnology*, 24(22), 225503/1–9.

Baumgartner, S., Vasicek, M., Bulyha, A., and Heitzinger, C. (2011a). Optimization of nanowire DNA sensor sensi-

tivity using self-consistent simulation. *Nanotechnology*, 22(42), 425503/1–8.

Baumgartner, S., Vasicek, M., and Heitzinger, C. (2011b). Analysis of field-effect biosensors using self-consistent 3D drift-diffusion and Monte-Carlo simulations. *Procedia Engineering*, 25, 407–410.

Baumgartner, S., Vasicek, M., and Heitzinger, C. (2012). Modeling and simulation of nanowire based field-effect biosensors. In G. Korotcenkov (ed.), *Chemical Sensors: Simulation and Modeling. Volume 2: Conductometric-Type Sensors*, 447–469. Momentum Press.

Bulyha, A. and Heitzinger, C. (2011). An algorithm for three-dimensional Monte-Carlo simulation of charge distribution at biofunctionalized surfaces. *Nanoscale*, 3(4), 1608–1617.

Das, S., Vikalo, H., and Hassibi, A. (2009). On scaling laws of biosensors: a stochastic approach. *Journal of Applied Physics*, 105(10), 102021.

Deen, M., Shinwari, M., Ranuárez, J., and Landheer, D. (2006). Noise considerations in field-effect biosensors. *Journal of applied physics*, 100(7), 074703.

Duan, X., Li, Y., Rajan, N.K., Routenberg, D.A., Modis, Y., and Reed, M.A. (2012). Quantification of the affinities and kinetics of protein interactions using silicon nanowire biosensors. *Nature nanotechnology*, 7(6), 401–407.

Erban, R., Chapman, J., and Maini, P. (2007). A practical guide to stochastic simulations of reaction-diffusion processes. *arXiv preprint arXiv:0704.1908*.

Gillespie, D.T. (2008). Simulation methods in systems biology. In *Formal Methods for Computational Systems Biology*, 125–167. Springer.

Hassibi, A., Navid, R., Dutton, R.W., and Lee, T.H. (2004). Comprehensive study of noise processes in electrode electrolyte interfaces. *Journal of applied physics*, 96(2), 1074–1082.

Hassibi, A., Vikalo, H., and Hajimiri, A. (2007). On noise processes and limits of performance in biosensors. *Journal of applied physics*, 102(1), 014909.

Hassibi, A., Zahedi, S., Navid, R., Dutton, R.W., and Lee, T.H. (2005). Biological shot-noise and quantum-limited signal-to-noise ratio in affinity-based biosensors. *Journal of Applied Physics*, 97(8), 084701.

Higham, D.J. (2008). Modeling and simulating chemical reactions. *SIAM review*, 50(2), 347–368.

Hunt, H.K. and Armani, A.M. (2010). Label-free biological and chemical sensors. *Nanoscale*, 2(9), 1544–1559.

Patolsky, F., Zheng, G., and Lieber, C. (2006). Fabrication of silicon nanowire devices for ultrasensitive, label-free, real-time detection of biological and chemical species. *Nature protocols*, 1(4), 1711–1724.

Stern, E., Klemic, J.F., Routenberg, D.A., Wyrembak, P.N., Turner-Evans, D.B., Hamilton, A.D., LaVan, D.A., Fahmy, T.M., and Reed, M.A. (2007). Label-free immunodetection with CMOS-compatible semiconducting nanowires. *Nature protocols*, 1(4), 1711–1724.

Stern, E., Vacic, A., Rajan, N.K., Criscione, J.M., Park, J., Ilic, B.R., Mooney, D.J., Reed, M.A., and Fahmy, T.M. (2010). Label-free biomarker detection from whole blood. *Nature nanotechnology*, 5(2), 138–142.

Tulzer, G., Baumgartner, S., Brunet, E., Mutinati, G.C., Steinhauer, S., Köck, A., Barbano, P.E., and Heitzinger, C. (2013). Kinetic parameter estimation and fluctuation

- analysis of CO at SnO₂ single nanowires. *Nanotechnology*, 24(31), 315501/1–10.
- Tulzer, G. and Heitzinger, C. (2014). Fluctuations due to association and dissociation processes at nanowire-biosensor surfaces and their optimal design. *Nanotechnology*, 26(2), 025502/1–9.
- Zheng, G., Patolsky, F., Cui, Y., Wang, W., and Lieber, C. (2005). Multiplexed electrical detection of cancer markers with nanowire sensor arrays. *Nature biotechnology*, 23(10), 1294–1301.